Am J Transl Res 2019;11(5):3101-3108
www.ajtr.org /ISSN:1943-8141/AJTR0091080

Original Article

Alterations in amino acid levels and metabolite ratio of spinal cord in rat with myocardial ischemia-reperfusion injury by proton magnetic resonance spectroscopy

Qian Wang[1], Zhi-Xiao Li[1], Yu-Juan Li[1], Anne Manyande[2], Shun-Yuan Li[3], Mao-Hui Feng[4], Duo-Zhi Wu[5], Hong-Bing Xiang[1]

[1]Departments of Anesthesiology and Pain Medicine, Tongji Hospital of Tongji Medical College, Huazhong University of Science and Technology, Wuhan 430030, Hubei, PR China; [2]School of Human and Social Sciences, University of West London, London, UK; [3]Department of Anesthesiology, The First Affiliated Quanzhou Hospital of Fujian Medical University, Quanzhou 362000, PR China; [4]Department of Gastrointestinal Surgery, Zhongnan Hospital, Wuhan University, No. 169 Donghu Road, Wuhan 430071, PR China; [5]Department of Anesthesiology, People's Hospital of Hainan Province, Haikou, Hainan, PR China

Received January 9, 2019; Accepted March 1, 2019; Epub May 15, 2019; Published May 30, 2019

Abstract: Objectives: The mechanism behind spinal metabolites and myocardial ischemia-reperfusion (IR) injury is not well understood. Proton magnetic resonance spectroscopic analysis of spinal cord extracts provides a quick evaluation of the specific metabolic activity in rats with myocardial IR injury. We investigated the relationship between the IR-related variables and the changes in spinal metabolites. Methods: Proton magnetic resonance spectroscopy (^{1}H-MRS) was used to assess the spinal metabolites of adult rats with and without myocardial IR injury (n = 6 per group). Myocardial IR injury was reproduced using intermittent occlusion of the left anterior descending coronary artery. We studied the relationship between the metabolite ratio measurement and IR-related variables. All rats underwent ^{1}H-MRS, with the ratio of interest placed in different spinal cord segments to measure levels of twelve metabolites including N-acetylaspartate (NAA), taurine (Tau), glutamate (Glu), gamma amino acid butyric acid (GABA), creatine (Cr), and myoinositol (MI), etc. Results: Rats with myocardial IR injury had higher concentration of Tau in the upper thoracic spinal cord ($P < 0.05$), and lower concentration of Gly and Glu in the cervical segment of the spinal cord ($P < 0.05$), when compared to the Control group. The ratios of glutamate/taurine (Glu/Tau), Glu/(GABA + Tau) and Glu/Total were significantly different between the IR group and the Control group in the upper thoracic spinal cord ($P < 0.05$). So were the ratios of Glu/(GABA + Tau) in the cervical segment ($P < 0.05$), and Glu/Tau and Glu/(GABA + Tau) in the lower thoracic spinal cord ($P < 0.05$). Conclusions: These findings suggest that myocardial IR injury may be related to spinal biochemical alterations. It is speculated that these observed changes in the levels of spinal metabolites may be involved in the pathogenesis and regulation of myocardial IR injury.

Keywords: Myocardial ischemia-reperfusion injury, spinal cord, metabolomics, proton nuclear magnetic resonance

Introduction

Cardiac ischemia reperfusion injury is a major risk factor for deaths in patients with cardiovascular disease [1-3]. A heart-spinal cord interaction has been described in cardiac ischemia [4] and related angina pectoris [5], but the mechanisms involved are unknown. Emerging research indicates that spinal cord stimulation (SCS) significantly alters the expression level of nociceptive transmitter in the spinal cord during cardiac ischemia resulting in coronary artery occlusion in rat models [6-9]. There is emerging evidence that peripheral nociceptive stimulation modulates spinal metabolism and cell growth in the spinal cord [10-13], and that spinal cellular adaptation to cardiac ischemic stress requires the coordination of cellular metabolic changes to maintain energy homeostasis [14, 15]. However, the associations between amino acid levels in the spinal cord and myocardial ischemia-reperfusion (IR) injury remain relatively unknown.

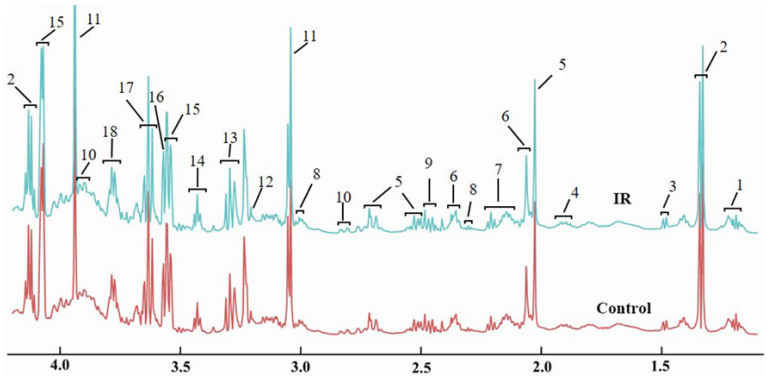

Figure 1. The normalized ^{1}H-NMR spectra of the Thoracic spinal cord samples (T1-T6) in control and IR groups. Note: 1, ethanol; 2, lactate; 3, alanine; 4, gamma amino acid butyric acid (GABA) + acetate; 5, N-aceytl aspartate (NAA); 6, glutamate; 7, glutamate + glutamine; 8, GABA; 9, glutamine; 10, asparate; 11, creatine; 12, choline; 13, taurine + myo-institol; 14, taurine; 15, myo-institol; 16, glycine; 17, ethanol + myo-institol; 18, alanine + glutamine + glutamate.

Only with a good understanding of the heart-spinal cord crosstalk can we develop optimal treatment regimen for patients with cardiac ischemia. Regrettably, the metabolic mechanism of the heart-spinal cord crosstalk remains unclear. Spinal cord neural-decoding that focuses on capturing chemical metabolic profiles from spinal activities faces great challenges. In recent years, spinal cord neural decoding with magnetic resonance imaging signals has resulted in numerous studies being conducted. Complex spinal cord activity with limited data instances make it necessary to analyze the correlations between chemical metabolic signals and nociceptive stimuli. We previously demonstrated specific patterns of metabolite changes in spinal cords after the intradermal microinjection of two different pruritogens (α-Me-5-HT and histamine) and one algogenic compound (capsaicin) using proton nuclear magnetic resonance spectroscopy (^{1}H-MRS) [16]. This work contributed knowledge about the working mechanism of the spinal cord neural decoding, and established the effective connectivity from peripheral nociceptive stimulation to chemical metabolic profiles in the spinal cord.

In the current study, we adopted a similar method of using ^{1}H-MRS to investigate the alterations of amino acid levels and metabolite ratio in rats' spinal cord with myocardial IR injury reproduced using intermittent occlusion of the left anterior descending coronary artery.

Material and methods

Animals

All experiments were performed in accordance with the guidelines of the Experimental Animal Laboratory and experimental protocols (TJ-A20-150804) approved by the Animal Care and Use Committee of Tongji Medical College, Huazhong University of Science and Technology. We used adult male SD rats (weighing 250-300 g) for our study. All animals were provided regular rat chow and water *ad libitum*, and were separately housed in a standard controlled environment (22 ± 1°C, 40-70% humidity, 12-h light/dark cycles).

Myocardial IR injury model in rats

Rats were divided randomly into two groups. For Group 1, the Control group (n = 6), rats underwent all surgical procedures except for left anterior descending coronary arterial (LAD) clamping. For Group 2, the IR group (n = 6), rats were exposed to the LAD clamp procedure. The myocardial IR was performed as described previously [17-21]. Briefly, the rats were anesthetized with 50 mg/kg ketamine and 7.5 mg/kg xylazine *i.p.* using a lamp to regulate body temperature (37 ± 1°C) through a heating pad. Then tracheal intubation was set up and the lungs were mechanically ventilated. A left thoracic incision was performed to expose the heart in the two groups, and LAD coronary artery was clamped to form a reversible trap for 30 min and induce ischemia. Ischemia was confirmed by the color of the heart. For reperfusion, the clamp was removed, and the heart was monitored for color change to confirm renewed blood flow before suturing the incision. After reperfusion for 2 h, the myocardial ischemic tissues were cut for histological and biochemical analyses whereas those from the spinal cord were collected for ^{1}H-MRS detection. The myocardial ischemic regions were prepared for Hematoxylin-Eosin (HE) and lower sections of the heart were incubated with 1% 2,3,5-Triphenyl

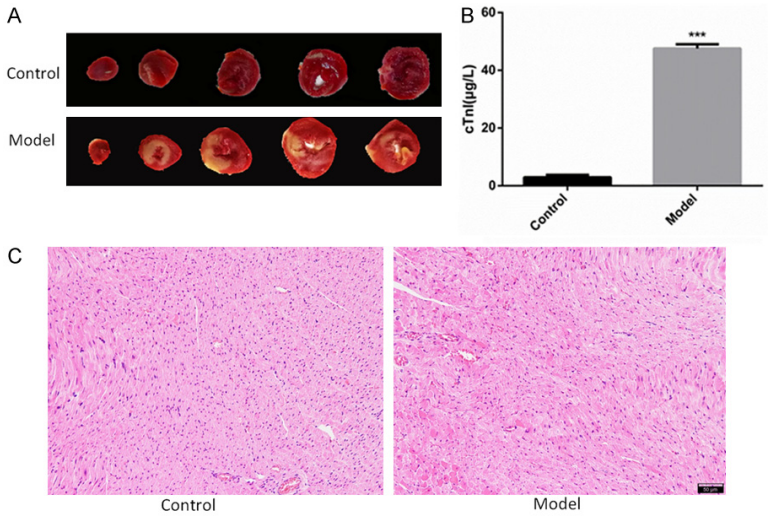

Figure 2. Evaluation of the myocardial I/R model. A. Representative photographs in hearts subjected to I/R injury. After incubated with 2,3,5-Triphenyl Tetrazolium Chloride (TTC), the pale part of the slice heart tissue represents the infarct area. B. Serum cTnI concentrations in rats with control or I/R injury. Values are means ± SEM, n = 4 rats per group. Mann-Whitney test. ***P < 0.001 vs. control group. C. Representative photographs of HE staining of heart sections. The left panel shows the Control group and the right panel shows the IR group. Scale bar = 50 μm.

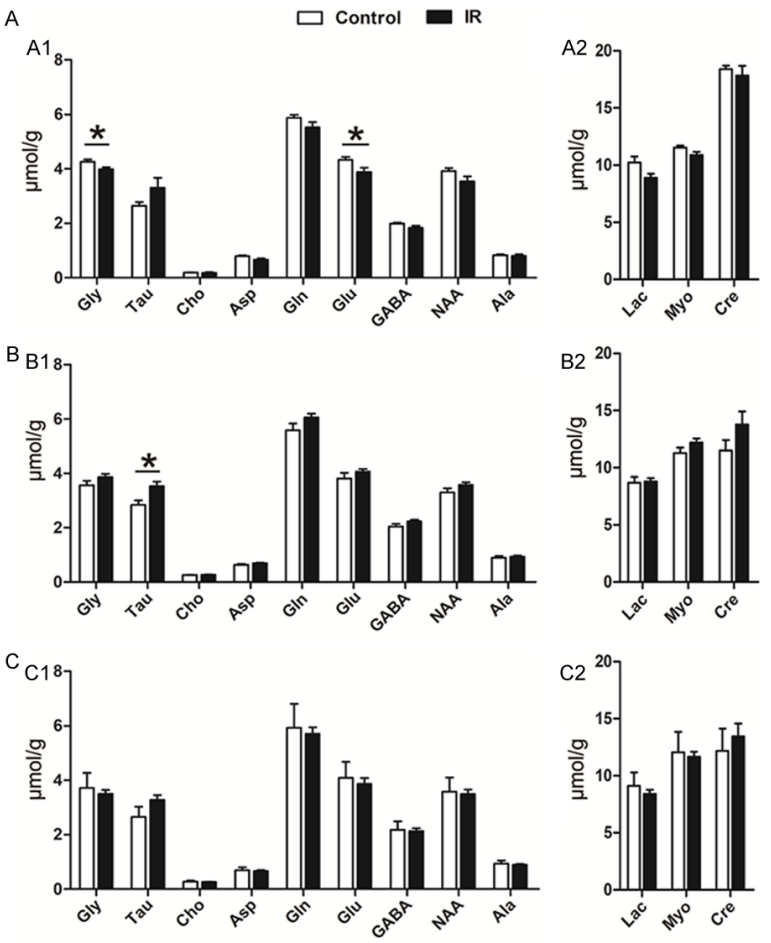

Figure 3. The concentration of identified metabolites in different parts of the spinal cord in control and ischemia reperfusion (IR) groups. A1, A2. The cervical segment of the rat spinal cord; B1, B2. The upper thoracic spinal cord (T1-T6); C1, C2. The lower thoracic spinal cord (T7-T12). Data is presented as means ± SEM. Mann-Whitney test. *P < 0.05. Note: Gly, glycine; Tau, taurine; Cho, choline; Asp, asparate; Gln, glutamine; Glu, glutamate; GABA, gamma amino acid butyric acid; NAA, N-aceytl aspartate; Ala, alanine; Lac, lactate; Myo, myo-institol; Cre, creatine.

Tetrazolium Chloride (TTC) for 10 min at 37°C. In addition, blood samples were obtained from the abdominal aorta to assess heart function.

Spinal cord sample for ^{1}H-MRS study and ^{1}H-MRS data processing

Protocols for spinal cord tissue extraction and ^{1}H-MRS spectrum acquirement were the same as those described in our previous study [16].

For NMR spectral data processing, the commercial software TOPSPIN and NMRSpec were used [22-24], and a home-made MATLAB code. All the spectra were manually phased and the baseline corrected in Topspin. The peak alignment and integration were completed in NMRSpec. The 18 related peak areas were calculated separately (**Figure 1**).

Statistical analysis

Statistical data are shown as the mean ± standard error of the mean (SEM). Analysis was performed using GraphPad Prism 6.0. Comparisons between the two groups were

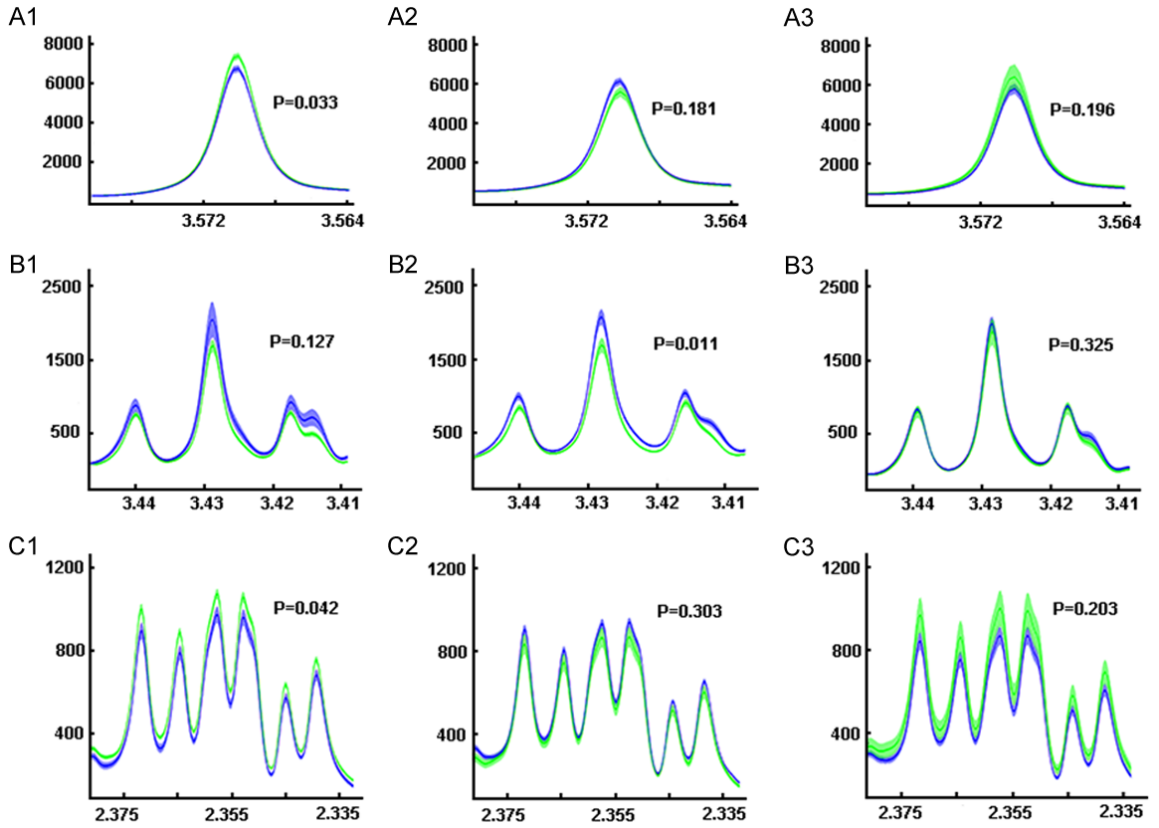

Figure 4. The average difference in normalized ^{1}H-NMR spectra of selected metabolites in control and ischemia reperfusion (IR) groups. A1-A3. The average spectra of glycine; B1-B3. The average spectra of taurine; C1-C3. The average spectra of glutamate. A1-C1. Represent the Cervical spinal cord; A2-C2. Represent the upper Thoracic spinal cord (T1-T6); A3-C3. Represent the lower Thoracic spinal cord (T7-T12). Note: the green line represents the average level and the green color surround means the SEM of the control group; the blue line represents the average level and the blue color surround means the SEM of the control group. The *p* value was calculated from the concentration of certain metabolites.

performed using the Mann-Whitney test. The *P* values of less than 0.05 were considered statistically significant.

Results

Evaluation of myocardial IR injury model

In this study, we used the histological and biochemical results to confirm the myocardial IR injury model. Representative images of TTC stained cross-sections of the heart are shown in **Figure 2A**. Serum cardiac troponin cTnI in the IR group was significantly increased compared to the Control group (**Figure 2B**). The results from HE staining show that the cardiac structural disorders were observed in the IR group, whereas myocardial cells in the control group were complete and arranged in order (**Figure 2C**).

Metabolic concentration and metabolic ratios in spinal cord extracts

In order to precisely assess the spinal changes after myocardial IR injury, absolute concentrations of all the related metabolites were calculated and compared (Tables S1-S3 and **Figure 3**). The average difference in normalized ^{1}H-NMR spectra of selected metabolites between control and IR groups are displayed in **Figure 4**.

Rats with myocardial IR injury had higher concentration of taurine (Tau) in the upper region of the thoracic spinal cord ($P < 0.05$) (**Figure 3B**; **Tables 1** and S1-S3), and lower concentration of glycine (Gly) and glutamate (Glu) in the cervical segment ($P < 0.05$) (**Figure 3A**; **Tables 1** and S1-S3), compared to the Control group.

Table 1. The concentration of selected metabolites in different segments of the spinal cord

Spinal Segment	Metabolite	Control (μmol/g)	IR (μmol/g)	P
C1-8	Glycine	4.26 ± 0.08	3.98 ± 0.08	**0.033**
	Taurine	2.65 ± 0.14	3.31 ± 0.37	0.127
	Glutamate	4.33 ± 0.11	3.88 ± 0.17	**0.042**
T1-6	Glycine	3.56 ± 0.17	3.86 ± 0.12	0.181
	Taurine	2.84 ± 0.16	3.53 ± 0.16	**0.011**
	Glutamate	3.81 ± 0.20	4.07 ± 0.10	0.303
T7-12	Glycine	3.72 ± 0.56	3.50 ± 0.15	0.196
	Taurine	2.65 ± 0.37	3.29 ± 0.17	0.325
	Glutamate	4.09 ± 0.59	3.87 ± 0.21	0.204

Note: C1-C8, the cervical segment of the rat spinal cord; T1-T6, the upper thoracic spinal cord; T7-T12, the lower thoracic spinal cord. Data was presented as means ± SEM. Mann-Whitney test. P < 0.05 was marked as bold.

Table 2. Comparisons of the spinal levels of the metabolic ratios of different groups

Spinal Segment	Metabolite Ratio	Control	IR	p
C1-8	Glu/Tau	1.70 ± 0.12	1.30 ± 0.13	0.052
	Glu/Total	0.49 ± 0.02	0.42 ± 0.02	**0.045**
	Glu/(GABA+Tau)	0.94 ± 0.04	0.78 ± 0.06	0.058
T1-6	Glu/Tau	1.37 ± 0.08	1.17 ± 0.04	**0.043**
	Glu/Total	0.45 ± 0.01	0.42 ± 0.01	**0.028**
	Glu/(GABA+Tau)	0.78 ± 0.03	0.71 ± 0.01	**0.048**
T7-12	Glu/Tau	1.56 ± 0.09	1.23 ± 0.11	**0.046**
	Glu/Total	0.48 ± 0.02	0.43 ± 0.02	0.104
	Glu/(GABA+Tau)	0.85 ± 0.03	0.72 ± 0.04	**0.041**

Note: C1-C8, the cervical segment of the rat spinal cord; T1-T6, the upper thoracic spinal cord; T7-T12, the lower thoracic spinal cord. Data was presented as means ± SEM. Mann-Whitney test. P < 0.05 was marked as bold.

Tables 2 and S1, S2, S3, S4, S5, S6 illustrate the comparisons of the mean levels of metabolite ratios between the two groups, and that rats in the IR group had lower levels of glutamate/taurine (Glu/Tau), Glu/(GABA + Tau) and Glu/Total than that of the Control group. Of note, the ratios of Glu/Tau, Glu/(GABA + Tau) and Glu/Total were significantly different between the groups in the upper thoracic spinal cord (P < 0.05) (**Figure 5B**; **Table 2**). So were the ratios of Glu/(GABA + Tau) in the cervical segment (P < 0.05) (**Figure 5A**; **Table 2**), and Glu/Tau and Glu/(GABA + Tau) in the lower thoracic spinal cord (P < 0.05) (**Figure 5C**; **Table 2**).

Discussion

The current study investigated the metabolic concentration and ratios in spinal cord extracts of rats with and without LAD ligation as assessed by ^{1}H-MRS, and compared the association of these variables in different spinal cord segments. The principal findings are as following: (1) LAD ligation resulted in myocardial IR injury; (2) The ^{1}H-MRS-measured Tau concentration in the upper thoracic spinal cord and exhibited a dramatic increase whereas Gly and Glu concentration of the cervical segment showed a significant decrease in the IR group; (3) Glu/(GABA + Tau) and Glu/Tau were significantly different between the groups in the upper thoracic spinal cord, indicating that in the spinal cord Glu/(GABA + Tau) and Glu/Tau are the surrogate markers of myocardial IR injury.

There is now substantial evidence that afferent feedback from the heart to the higher centres may affect efferent input to the heart and modulate cardiac physiology [25]. The rapid development of ^{1}H-MRS could detect and quantify hundreds of proteins and metabolites [26, 27], which are located downstream of the entire biology system, and represent the direct performance of the life system and final feedback of the overall biological processes. We found that the ^{1}H-MRS-measurement of Tau concentration in the T1-T6 spinal cord exhibited a dramatic increase in the IR group. As an inhibitory amino acid, Tau (2-aminoethanesulfonic acid) plays an important role in the maintenance of calcium homeostasis, membrane stabilization, antioxidation, and antiinflammatory action [28-30]. Smullin reported that Tau release in response to chemical tests of nociception may contribute to the effective endogenous antinociceptive effect [28]. Some studies confirmed that Tau had protective effects against early renal injury in several animal models with potent endogenous antioxidative properties [31-33]. Cavdar investigated the effects of Tau and the possible role of p38 MAPK signaling

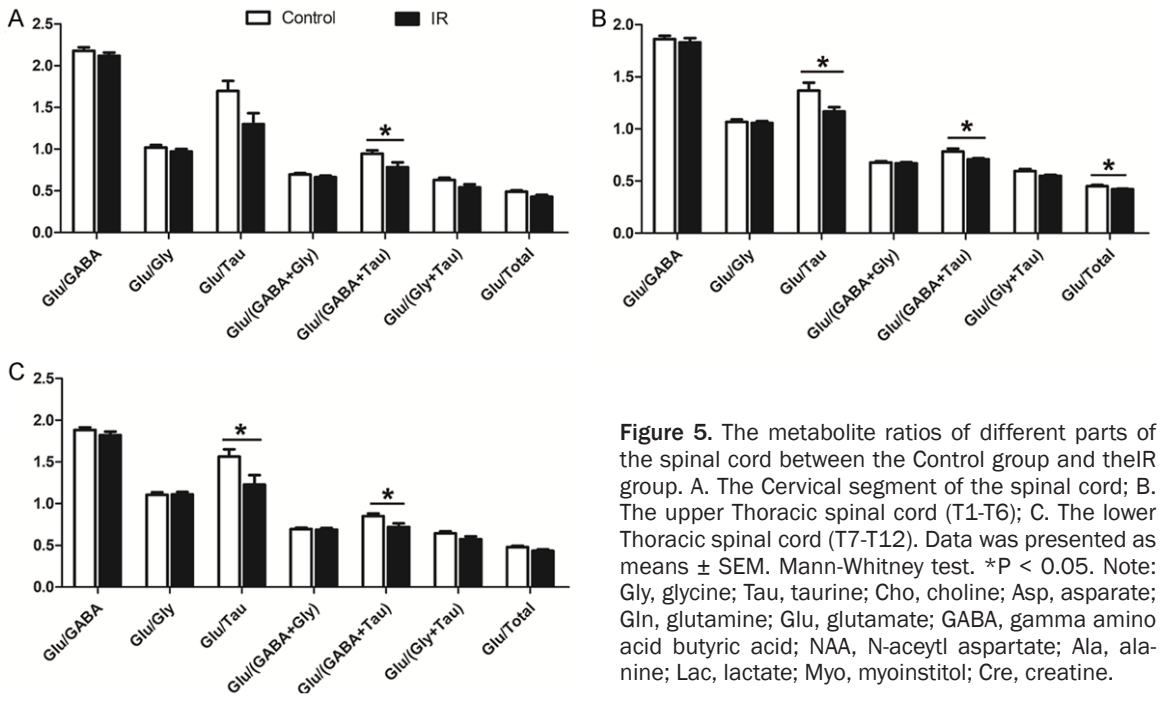

Figure 5. The metabolite ratios of different parts of the spinal cord between the Control group and theIR group. A. The Cervical segment of the spinal cord; B. The upper Thoracic spinal cord (T1-T6); C. The lower Thoracic spinal cord (T7-T12). Data was presented as means ± SEM. Mann-Whitney test. *P < 0.05. Note: Gly, glycine; Tau, taurine; Cho, choline; Asp, asparate; Gln, glutamine; Glu, glutamate; GABA, gamma amino acid butyric acid; NAA, N-aceytl aspartate; Ala, alanine; Lac, lactate; Myo, myoinstitol; Cre, creatine.

on the regulation of MMP-2 and MMP-9 in a renal IR injury model in rats, and found that Tau administration may prove to be a strategy for attenuating renal IR injury [31]. Thus, these data could further explain the mechanism behind the significantly higher Tau in the spinal cord related to myocardial IR injury. Besides, Taurine is closely related to neural cell damage [34]. We noticed that absolute Taurine concentration in the spinal tissue was much lower than normal animals. However, the experimental animals undergoing the procedures were much different from normal animals. So we could not exclude that the effects of the experimental operation itself will distinguish the results from naive animals, which needs further study.

Despite the existence of published mathematical techniques for ^{1}H-MRS-measuring absolute quantification, relative metabolite ratios are valid and useful. Region specific changes in relative metabolite ratios, such as NAA/Cr, Cho/Cr, and NAA/Cho have been found in a number of different neurological conditions. Widerström-Noga et al first reported a method to detect the ^{1}H-MRS in the anterior cingulate cortex and they found that glutamate-glutamine/myoinositol (Glx/Ins) ratio might be a useful biomarker for severe SCI-related neuropathic pain with significant psychosocial impact [35]. By using a similar method, Wang et al reported low levels of NAA/Cr and Cho/Cr in the hypothalamus of patients with episodic cluster headaches, suggesting that cluster headaches might be related to both neuronal dysfunction and changes in membrane lipids in the hypothalamus [36]. ^{1}H-MRS metabolite ratios measured in this study showed that Glu/(GABA + Tau) and Glu/Tau were significantly different between the IR group and Control group in the upper thoracic spinal cord, suggesting metabolic changes of excitatory and inhibitory amino acids in the spinal cord.

In conclusion, this study demonstrated that myocardial ischemia-reperfusion injury affected the tissue levels of amino acids and their ratios in the investigated spinal cord regions, suggesting that alterations in the spinal metabolisms of amino acids associated with myocardial ischemia-reperfusion injury are involved in the effects of central regulation.

Acknowledgements

This work was supported in part by grants from the National Natural Science Foundation of China (No. 81873467, 81670240, 81770283, 81072152) and the Clinical Medical Research Center of Peritoneal Cancer of Wuhan (No. 201506091-1020462) and the Natural Scien-

ce Foundation of Hubei Province (No. 2015-CFA027), the Research Foundation of Health and Family Planning Commission of Hubei Province (No. WJ2015MA010, WJ2017M249), Medical innovation project in Fujian Province (No. 2017-CX-48) and the Key Research and Development Project of Hainan Province of China (ZDYF2018115 to D.Z.W).

Disclosure of conflict of interest

None.

Address correspondence to: Dr. Mao-Hui Feng, Department of Gastrointestinal Surgery, Zhongnan Hospital, Wuhan University, No. 169 Donghu Road, Wuhan 430071, Hubei, PR China. E-mail: fengmh-5690@163.com; Dr. Hong-Bing Xiang, Department of Anesthesiology and Pain Medicine, Tongji Hospital, Tongji Medical College, Huazhong University of Science and Technology, Wuhan 430030, Hubei, PR China. E-mail: xhbtj2004@163.com

References

[1] Cheng YF, Chang YT, Chen WH, Shih HC, Chen YH, Shyu BC and Chen CC. Cardioprotection induced in a mouse model of neuropathic pain via anterior nucleus of paraventricular thalamus. Nat Commun 2017; 8: 826.

[2] Roth GA, Huffman MD, Moran AE, Feigin V, Mensah GA, Naghavi M and Murray CJ. Global and regional patterns in cardiovascular mortality from 1990 to 2013. Circulation 2015; 132: 1667-1678.

[3] Hausenloy DJ and Yellon DM. Myocardial ischemia-reperfusion injury: a neglected therapeutic target. J Clin Invest 2013; 123: 92-100.

[4] Osborn JW and Fink GD. Region-specific changes in sympathetic nerve activity in angiotensin II-salt hypertension in the rat. Exp Physiol 2010; 95: 61-68.

[5] Singh H, Merry AF, Ruygrok P and Ruttley A. Treatment of recurrent chest pain in a heart transplant recipient using spinal cord stimulation. Anaesth Intensive Care 2008; 36: 242-244.

[6] Di Pede F, Zuin G, Giada F, Pinato G, Turiano G, Bevilacqua M, Cazzin R and Raviele A. Long-term effects of spinal cord stimulation on myocardial ischemia and heart rate variability: results of a 48-hour ambulatory electrocardiographic monitoring. Ital Heart J 2001; 2: 690-695.

[7] Hautvast RW, Blanksma PK, DeJongste MJ, Pruim J, van der Wall EE, Vaalburg W and Lie KI. Effect of spinal cord stimulation on myocardial blood flow assessed by positron emission tomography in patients with refractory angina pectoris. Am J Cardiol 1996; 77: 462-467.

[8] Howard-Quijano K, Takamiya T, Dale EA, Kipke J, Kubo Y, Grogan T, Afyouni A, Shivkumar K and Mahajan A. Spinal cord stimulation reduces ventricular arrhythmias during acute ischemia by attenuation of regional myocardial excitability. Am J Physiol Heart Circ Physiol 2017; 313: H421-H431.

[9] Hautvast RW, Ter Horst GJ, DeJong BM, DeJongste MJ, Blanksma PK, Paans AM and Korf J. Relative changes in regional cerebral blood flow during spinal cord stimulation in patients with refractory angina pectoris. Eur J Neurosci 1997; 9: 1178-1183.

[10] He ZG, Liu BW, Li ZX, Liu C and Xiang HB. Altered expression profiling of spinal genes modulated by compound 48/80 in a mouse itch model. J Anesth Perioper Med 2017; 4: 220-224.

[11] Liu BW, Li ZX, He ZG, Liu C, Xiong J and Xiang HB. Altered expression of target genes of spinal cord in different itch models compared with capsaicin assessed by RT-qPCR validation. Oncotarget 2017; 8: 74423-74433.

[12] Wang Q, Li ZX, Liu BW, He ZG, Liu C, Chen M, Liu SG, Wu WZ and Xiang HB. Altered expression of differential gene and lncRNA in the lower thoracic spinal cord on different time courses of experimental obstructive jaundice model accompanied with altered peripheral nociception in rats. Oncotarget 2017; 8: 106098-106112.

[13] Ye DW, Liu C, Liu TT, Tian XB and Xiang HB. Motor cortex-periaqueductal gray-spinal cord neuronal circuitry may involve in modulation of nociception: a virally mediated transsynaptic tracing study in spinally transected transgenic mouse model. PLoS One 2014; 9: e89486.

[14] Zaha VG and Young LH. AMP-activated protein kinase regulation and biological actions in the heart. Circ Res 2012; 111: 800-814.

[15] Qi D, Atsina K, Qu L, Hu X, Wu X, Xu B, Piecychna M, Leng L, Fingerle-Rowson G, Zhang J, Bucala R and Young LH. The vestigial enzyme D-dopachrome tautomerase protects the heart against ischemic injury. J Clin Invest 2014; 124: 3540-3550.

[16] Liu T, He Z, Tian X, Kamal GM, Li Z, Liu Z, Liu H, Xu F, Wang J and Xiang H. Specific patterns of spinal metabolites underlying alpha-Me-5-HT-evoked pruritus compared with histamine and capsaicin assessed by proton nuclear magnetic resonance spectroscopy. Biochim Biophys Acta 2017; 1863: 1222-1230.

[17] Murry CE, Jennings RB and Reimer KA. Preconditioning with ischemia: a delay of lethal cell injury in ischemic myocardium. Circulation 1986; 74: 1124-1136.

[18] Huang CH, Lai CC, Yang AH and Chiang SC. Myocardial preconditioning reduces kidney injury and apoptosis induced by myocardial ischaemia and reperfusion. Eur J Cardiothorac Surg 2015; 48: 382-391.
[19] Borst O, Ochmann C, Schonberger T, Jacoby C, Stellos K, Seizer P, Flogel U, Lang F and Gawaz M. Methods employed for induction and analysis of experimental myocardial infarction in mice. Cell Physiol Biochem 2011; 28: 1-12.
[20] Pisarenko OI, Shulzhenko VS, Studneva IM, Serebryakova LI, Pelogeykina YA and Veselova OM. Signaling pathways of a structural analogue of apelin-12 involved in myocardial protection against ischemia/reperfusion injury. Peptides 2015; 73: 67-76.
[21] Wang Q, He ZG, Li ZX, Li SY, Chen YL, Feng MH, Hong QX and Xiang HB. Bioinformatics analysis of gene expression profile data to screen key genes involved in cardiac ischemia-reperfusion injury. Int J Clin Exp Med 2018; 11: 4955-4966.
[22] Liu Y, Cheng J, Liu HL, Deng YH, Wang J and Xu FQ. NMRSpec: an integrated software package for processing and analyzing one dimensional nuclear magnetic resonance spectra. Chemometr Intell Lab Syst 2017; 162: 142-148.
[23] Farag MA, Mahrous EA, Lubken T, Porzel A and Wessjohann L. Classification of commercial cultivars of humulus lupulus L. (hop) by chemometric pixel analysis of two dimensional nuclear magnetic resonance spectra. Metabolomics 2014; 10: 21-32.
[24] Geil B, Diezemann G and Bohmer R. Stimulated echoes and two-dimensional nuclear magnetic resonance spectra for solids with simple line shapes. J Chem Phys 2008; 128: 114506.
[25] Mazzeo AT, Micalizzi A, Mascia L, Scicolone A and Siracusano L. Brain-heart crosstalk: the many faces of stress-related cardiomyopathy syndromes in anaesthesia and intensive care. Br J Anaesth 2014; 112: 803-815.
[26] Zeng HL, Yang Q, Du H, Li H, Shen Y, Liu T, Chen X, Kamal GM, Guan Q, Cheng L, Wang J and Xu F. Proteomics and metabolomics analysis of hepatic mitochondrial metabolism in alcohol-preferring and non-preferring rats. Oncotarget 2017; 8: 102020-102032.
[27] Chen R and Snyder M. Promise of personalized omics to precision medicine. Wiley Interdiscip Rev Syst Biol Med 2013; 5: 73-82.
[28] Smullin DH, Skilling SR and Larson AA. Interactions between substance P, calcitonin gene-related peptide, taurine and excitatory amino acids in the spinal cord. Pain 1990; 42: 93-101.
[29] Kurachi M, Yoshihara K and Aihara H. Effect of taurine on depolarizations induced by L-glutamate and other excitatory amino acids in the isolated spinal cord of the frog. Jpn J Pharmacol 1983; 33: 1247-1254.
[30] Gupta RC, Seki Y and Yosida J. Role of taurine in spinal cord injury. Curr Neurovasc Res 2006; 3: 225-235.
[31] Cavdar Z, Ural C, Celik A, Arslan S, Terzioglu G, Ozbal S, Yildiz S, Ergur UB, Guneli E, Camsari T and Akdogan G. Protective effects of taurine against renal ischemia/reperfusion injury in rats by inhibition of gelatinases, MMP-2 and MMP-9, and p38 mitogen-activated protein kinase signaling. Biotech Histochem 2017; 92: 524-535.
[32] Wang L, Zhang L, Yu Y, Wang Y and Niu N. The protective effects of taurine against early renal injury in STZ-induced diabetic rats, correlated with inhibition of renal LOX-1-mediated ICAM-1 expression. Ren Fail 2008; 30: 763-771.
[33] Chiba Y, Ando K and Fujita T. The protective effects of taurine against renal damage by salt loading in Dahl salt-sensitive rats. J Hypertens 2002; 20: 2269-2274.
[34] Saransaari P and Oja SS. Taurine and neural cell damage. Amino Acids 2000; 19: 509-526.
[35] Widerstrom-Noga E, Pattany PM, Cruz-Almeida Y, Felix ER, Perez S, Cardenas DD and Martinez-Arizala A. Metabolite concentrations in the anterior cingulate cortex predict high neuropathic pain impact after spinal cord injury. Pain 2013; 154: 204-212.
[36] Wang SJ, Lirng JF, Fuh JL and Chen JJ. Reduction in hypothalamic 1H-MRS metabolite ratios in patients with cluster headache. J Neurol Neurosurg Psychiatry 2006; 77: 622-625.

Table S1. The concentration of selected metabolites in different segments of C1-C8

Metabolite	Control (μmol/g)	IR (μmol/g)	P
Cretine	18.40 ± 0.30	17.84 ± 0.84	0.561
Glycine	4.26 ± 0.08	3.98 ± 0.08	0.033
Myo-Ins	11.54 ± 0.18	10.89 ± 0.29	0.084
Taurine	2.65 ± 0.14	3.31 ± 0.37	0.127
Choline	0.19 ± 0.01	0.18 ± 0.02	0.641
Asparate	0.79 ± 0.03	0.66 ± 0.05	0.055
Glutamine	5.88 ± 0.11	5.52 ± 0.19	0.149
Glutamate	4.33 ± 0.11	3.88 ± 0.17	0.042
GABA	1.99 ± 0.04	1.84 ± 0.08	0.124
NAA	3.92 ± 0.11	3.54 ± 0.19	0.115
Alanine	0.82 ± 0.04	0.80 ± 0.06	0.748
Lactate	10.25 ± 0.51	8.89 ± 0.35	0.054

Table S2. The concentration of selected metabolites in different segments of T1-6

Metabolite	Control (μmol/g)	IR (μmol/g)	P
Cretine	11.50 ± 0.92	13.78 ± 1.15	0.161
Glycine	3.56 ± 0.17	3.86 ± 0.12	0.181
Myo-Ins	11.28 ± 0.48	12.20 ± 0.35	0.157
Taurine	2.84 ± 0.16	3.53 ± 0.16	0.011
Choline	0.26 ± 0.01	0.27 ± 0.01	0.487
Asparate	0.64 ± 0.03	0.69 ± 0.02	0.166
Glutamine	5.59 ± 0.25	6.05 ± 0.14	0.138
Glutamate	3.81 ± 0.20	4.07 ± 0.10	0.303
GABA	2.04 ± 0.10	2.23 ± 0.06	0.152
NAA	3.30 ± 0.15	3.58 ± 0.09	0.151
Alanine	0.90 ± 0.06	0.93 ± 0.04	0.617
Lactate	8.68 ± 0.51	8.79 ± 0.30	0.863

Table S3. The concentration of selected metabolites in different segments of T7-10

Metabolite	Control (μmol/g)	IR (μmol/g)	P
Cretine	12.18 ± 1.93	13.44 ± 1.13	0.965
Glycine	3.72 ± 0.56	3.50 ± 0.15	0.196
Myo-Ins	12.06 ± 1.77	11.66 ± 0.43	0.249
Taurine	2.65 ± 0.37	3.29 ± 0.17	0.325
Choline	0.28 ± 0.04	0.26 ± 0.01	0.117
Asparate	0.70 ± 0.10	0.66 ± 0.04	0.200
Glutamine	5.93 ± 0.87	5.71 ± 0.24	0.244
Glutamate	4.09 ± 0.59	3.87 ± 0.21	0.203
GABA	2.18 ± 0.32	2.13 ± 0.10	0.303
NAA	3.58 ± 0.52	3.49 ± 0.17	0.285
Alanine	0.94 ± 0.12	0.90 ± 0.02	0.104
Lactate	9.11 ± 1.19	8.39 ± 0.37	0.063

Table S4. Comparisons of the levels of the metabolic ratios of different groups in C1-8

Metabolic ratio	Control	IR	P
Glu/GABA	2.178 ± 0.042	2.119 ± 0.038	0.330
Glu/Gly	1.019 ± 0.029	0.971 ± 0.031	0.295
Glu/Tau	1.696 ± 0.123	1.300 ± 0.133	0.052
Glu/(GABA + Gly)	0.694 ± 0.017	0.664 ± 0.016	0.250
Glu/(GABA + Tau)	0.944 ± 0.042	0.784 ± 0.057	0.045
Glu/(Gly + Tau)	0.631 ± 0.024	0.543 ± 0.034	0.063
Glu/Total	0.489 ± 0.016	0.429 ± 0.023	0.058

Table S5. Comparisons of the levels of the metabolic ratios of different groups in T1-6

Metabolic ratio	Control	IR	P
Glu/GABA	1.861 ± 0.031	1.830 ± 0.042	0.575
Glu/Gly	1.068 ± 0.023	1.056 ± 0.020	0.717
Glu/Tau	1.368 ± 0.077	1.167 ± 0.042	0.043
Glu/(GABA + Gly)	0.678 ± 0.013	0.669 ± 0.011	0.605
Glu/(GABA + Tau)	0.783 ± 0.027	0.708 ± 0.014	0.028
Glu/(Gly + Tau)	0.596 ± 0.019	0.551 ± 0.009	0.055
Glu/Total	0.451 ± 0.012	0.423 ± 0.005	0.048

Table S6. Comparisons of the levels of the metabolic ratios of different groups in T7-10

Metabolic ratio	Control	IR	P
Glu/GABA	1.882 ± 0.035	1.822 ± 0.041	0.324
Glu/Gly	1.108 ± 0.028	1.109 ± 0.033	0.984
Glu/Tau	1.564 ± 0.086	1.229 ± 0.114	0.046
Glu/(GABA + Gly)	0.697 ± 0.015	0.689 ± 0.018	0.752
Glu/(GABA + Tau)	0.850 ± 0.032	0.720 ± 0.043	0.041
Glu/(Gly + Tau)	0.645 ± 0.023	0.574 ± 0.033	0.119
Glu/Total	0.480 ± 0.015	0.434 ± 0.020	0.104